

# Experimental determination of the nucleation probability in emulsions

S. Gibout\*, A. Jamil, T. Kousksou, Y. Zéraouli, J. Castaing-Lasvignottes

*Laboratoire de Thermique Énergétique et Procédés, Avenue de l'Université, BP 1155, 64013 PAU Cedex, France*

Received 22 June 2006; received in revised form 11 December 2006; accepted 11 December 2006

Available online 20 December 2006

## Abstract

We present in this paper a new method of determining the nucleation probability  $J(T)$  of a supercooled liquid dispersed within an emulsion, based on the analysis of the thermogram obtained during a regular cooling. The thermal behaviour of the sample during the cooling is modelled in order to calculate the thermogram and so to compare it with the experimental thermogram. A genetic algorithm (GA) is then used to identify the parameters of the  $J(T)$  function by minimizing a least squares objective function comparing calculated and measured thermograms. This identification procedure is used to determine the crystallization probability of two samples of same composition but of different manufacture. The results are compared with each other as well as with the results obtained through a traditional calorimetric method. These various tests show that GA associated with calorimetry is a useful and easy tool for the determination of the nucleation probability  $J(T)$ .

© 2006 Elsevier B.V. All rights reserved.

*Keywords:* Emulsion; Supercooling; Nucleation probability; Genetic algorithm (GA); Differential scanning calorimetry (DSC)

## 1. Introduction

Fusion and crystallization of a pure substance are two non-symmetrical phenomena: whereas fusion always occurs at the melting point  $T_F$ , crystallization may happen at a temperature  $T_C$  lower than  $T_F$ . It is the undercooling (also called supercooling) phenomenon [1].

The metastability breakdown – which leads to crystallization – is a random phenomenon that must be described in terms of probability. One introduces the probability of crystallization per unit of time  $J(T)$  which represents an important information for the examination of undercooling and is essential to model the thermal behaviour of a liquid when being cooled below its melting point [2,3].

Although the theoretical form of  $J(T)$  is known [4,5], it is often necessary to determine it out of from experimental data. The most widely used methods are based on the analysis of thermograms recorded during a steady cooling [6]. These methods generally suppose that the temperature of the sample is uniform and equal to the programmed temperature, what is generally false. Moreover, the determination of  $J$  for a range of temperatures requires several cooling–heating cycles, which can damage the emulsion.

To avoid these various difficulties, we have developed a method based on an opposite approach [7,8] with the identification of several parameters of a 2D unsteady heat transfer model. Although the results show the validity of this method, the experimentations are fastidious and time-consuming (about 10 h) and require a large quantity of sample (about 100 ml).

We present in this paper a new “hybrid” identification method based on the use of genetic algorithms for the analysis of thermograms obtained by calorimetry. It allows to work with a very small quantity of sample (a few milligrams). Besides, the method does not require several heating–cooling cycles, allowing the study of fragile emulsions. However, this method has to be reserved to the emulsions whose only the dispersed phase crystallizes. This restriction has several consequences on the assumptions that can be formulated concerning the crystallization kinetics and the heat transfer model. Furthermore, the expression of  $J(T)$  supposes that all the droplets have the same volume. This rigorously limits the application fields of the method to strictly monodisperses emulsions. We will reconsider these various points in the following paragraphs.

## 2. Crystallization kinetics of droplets dispersed within an emulsion

Due to the undercooling phenomenon, crystallization of a substance occurs at a temperature  $T_C$  lower than the melting

\* Corresponding author. Tel.: +33 559407720; fax: +33 559407725.

E-mail address: [stephane.gibout@univ-pau.fr](mailto:stephane.gibout@univ-pau.fr) (S. Gibout).

point  $T_F$ . For a given substance the undercooling  $\Delta T = T_F - T_C > 0$  mainly depends on the sample volume [9]: typically values of  $\Delta T$  for water are 14 K for volume of a few  $\text{mm}^3$  and 39 K for volume about  $\mu\text{m}^3$  [2].

It is however important to note that  $\Delta T$  is a statistical data since the metastability breakdown is a fundamentally random process [1,10].

The crystallization process can be seen as a two steps process [11,12]. The first one corresponds to the apparition within the liquid phase of a “supercritical aggregate” having the same crystalline structure as the solid. It is the “germination” or “nucleation” phase. The second phase corresponds to the crystalline growth, initiated by this supercritical germ and leading to the total crystallization of the sample.

In this work, we are interested in the crystallization of the droplets dispersed within an emulsion. As their average size is close to the micrometer and the liquid is undercooled, i.e. far from its stable state, we consider the crystalline growth as instantaneous. Thus, the kinetics of crystallization is assumed to be exclusively driven by the germination phase [13]. Then the complete crystallization of the sample occurs when the first supercritical aggregate appears.

The classical theories of nucleation [4,5,14,15] define the probability of nucleation per unit volume and unit volume  $I(T)$ , which corresponds to the probability of formation of the supercritical aggregate initiating crystallization:

$$I(T) = k(T) \exp\left(-\frac{\Delta G^*}{kT}\right) \quad (1)$$

The work of formation of the supercritical aggregate  $\Delta G^*$  is mainly due to the surface tension  $\sigma$  between the liquid and the aggregate. During its formation within the liquid (homogeneous nucleation), the work of formation of the supercritical aggregate is given by the following expression [4,16]:

$$\Delta G^* = \frac{16}{3} \frac{\sigma^3 v^2}{\ell_F^2} \left(\frac{T_F}{T_F - T}\right)^2 \quad (2)$$

with  $v$  is the molar volume of the liquid and  $\ell_F$  is the molar heat of fusion. The pre-exponential term  $k(T)$  varies more slowly with the temperature than the exponential term and can be thus considered as constant in this work.

For a single droplet of size  $V$ , the probability of nucleation per unit time  $J(T) = VI(T)$  may be expressed as

$$J(T) = \begin{cases} A \exp\left(-\frac{B}{T(T - T_F)^2}\right) & \text{for } T < T_F \\ 0 & \text{for } T \geq T_F \end{cases} \quad (3)$$

where  $A = Vk(T)$  and  $B = (16/3)(\sigma^3 v^2 T_F^2 / k \ell_F^2)$  are considered as constants for a given volume  $V$ . The  $B$  coefficient is a characteristic of the undercooled substance (molar volume of the crystal, liquid-crystal interfacial tension) whereas  $A$  linearly depends on the volume of the crystal [17,9,18,1,4] for the case of heterogeneous nucleation.

As we suppose here that the crystalline growth is instantaneous and begins with the formation of the first supercritical aggregate,  $J(T)$  also represents the probability of crystalliza-

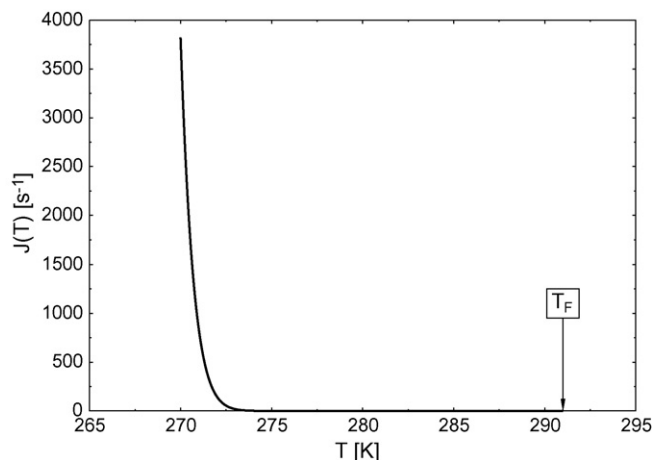


Fig. 1. Probability of crystallization per unit time  $J(T)$  for  $A = 1.8 \times 10^{10} \text{ s}^{-1}$ ,  $B = 1.6 \times 10^6 \text{ K}^3$  and  $T_F = 291 \text{ K}$ .

tion per unit time of a droplet of volume  $V$ . The  $J(T)$  function is strongly nonlinear. It remains very close to zero for a wide range of temperatures below  $T_F$  and then quickly increases when  $T$  decreases (see Fig. 1).

### 2.1. Case of a droplet population

Due to the stochastic nature of metastability breakdown, it is necessary to use a statistical approach, simultaneously studying a large number of samples. This can be done by considering the droplets of a near monodisperse emulsion.

Let  $n_t$  be the total number of droplets per unit volume of emulsion and  $n$  the number of crystallized droplets. Between times  $t$  and  $t + dt$ , whereas the temperature is assumed to be constant, the rate of crystallizing droplets can be expressed as the product of the number of liquid droplets  $n_t - n$  and the crystallization probability  $J(T)$ :

$$\frac{dn}{dt} = (n_t - n)J(T) \quad (4)$$

Introducing the crystallized fraction  $\phi = n/n_t$ , Eq. (4) can be rewritten as

$$\frac{d\phi}{dt} = (1 - \phi)J(T) \quad (5)$$

This expression constitutes the fundamental equation of the kinetics of the crystallization of the droplets dispersed within an emulsion.

## 3. Numerical simulation of emulsion cooling inside the calorimetric cell

The thermal behaviour of an emulsion enclosed inside a DSC cell has already been examined [8,19]. In particular, a transient 2D axi-symmetrical model was designed [20]. This model requires the knowledge of all the thermophysical properties, including the thermal conductivity and  $J(T)$  which are difficult to determine. It is also necessary to define the exact geometry of the sample, that may be difficult because of the small size of the cell and the induced capillarity phenomenon.

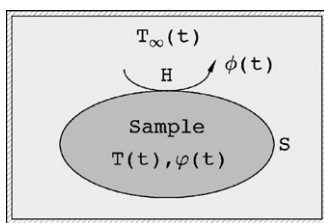


Fig. 2. Simplified model of the sample in the calorimetric cell.

In this work, we use a simplified lumped transient model. In spite of the imposed constraints that will be detailed hereafter, this method allows to avoid the problems previously mentioned. Moreover since the model is now simplified, the computing times are reduced.

The model represents the sample holder filled with an amount  $m$  of emulsion (cf. Fig. 2). Its state is characterized by its temperature  $T(t)$  and its crystallized fraction  $\varphi(t)$ , which evolve in time. The cooling of the sample is imposed by the circulation of a fluid around the cell. The temperature of this cooling fluid is denoted by  $T_\infty(t)$ . The outer area of the sample is  $S$  and the corresponding global heat exchange coefficient is  $H$ .

The emulsion is treated as an homogeneous medium characterized by its density  $\rho$ , its heat capacity  $C$  and its heat of crystallization per unit mass  $L$ . Since only the dispersed phase crystallizes, we have  $L = PL_F$  where  $P$  is the mass fraction (i.e. mass of dispersed phase divided by the total mass of the sample) and  $L_F$  the latent heat of crystallization of the dispersed phase. Let us note that only  $L$  is directly accessible by calorimetry.

The heat capacity is assumed to be linearly dependent on the crystallized fraction  $\varphi$ :

$$C(\varphi) = C_L + (C_S - C_L)\varphi(t) \quad (6)$$

where  $C_L$  is the heat capacity of the emulsion when droplets are in the liquid, and  $C_S$  is the heat capacity of the emulsion when droplets are in the solid state.

Because the heat conduction within the emulsion is not taken into account, the homogeneity of temperature within the sample must be taken as given. This imposes particularly a low cooling rate and a small amount of sample [21].

With the previous hypotheses, the first law of thermodynamics applied to the sample leads to:

$$mC \frac{dT(t)}{dt} = HS(T_\infty(t) - T(t)) + mL \frac{d\varphi(t)}{dt} \quad (7)$$

plus Eq. (5) describing the crystallization kinetics:

$$\frac{d\varphi(t)}{dt} = (1 - \varphi(t))J(T(t)) \quad (8)$$

In the Eq. (7),  $\phi_{\text{sim}}(t) = HS(T_\infty(t) - T(t))$  represents the heat flow received by the sample. This quantity corresponds to the information  $\phi_{\text{exp}}(t)$  provided by the DSC.

At  $t = 0$ , we assume that the sample is in thermal equilibrium with the calorimeter  $T(0) = T_\infty(0)$  and that all droplets are in the liquid state  $\varphi(0) = 0$ .

The Eqs. (7) and (8) are solved using the classical explicit Euler method with constant time step  $\Delta t$ .

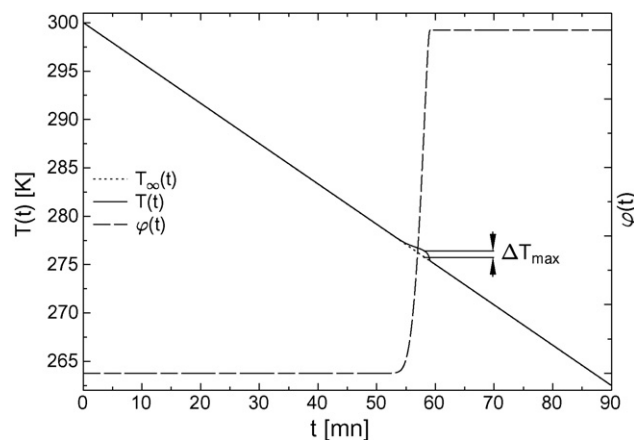


Fig. 3. Simulated evolution of  $T(t)$  and  $\varphi(t)$ .

Fig. 3 shows the evolution of the temperature  $T(t)$  and of the crystallized fraction  $\varphi(t)$  during a steady cooling ( $\beta = -0.5 \text{ K min}^{-1}$ ). The characteristics of the sample are:  $\rho = 1000 \text{ kg m}^{-3}$ ,  $C_L = 2500 \text{ J kg}^{-1} \text{ K}^{-1}$ ,  $C_S = 2000 \text{ J kg}^{-1} \text{ K}^{-1}$ ,  $L = 100 \text{ kJ kg}^{-1}$ ,  $T_F = 291 \text{ K}$ ,  $A = 1.8 \times 10^{10} \text{ s}^{-1}$ ,  $B = 1.6 \times 10^6 \text{ K}^3$ ,  $m = 10 \times 10^{-6} \text{ kg}$  and  $HS = 0.01 \text{ W K}^{-1}$ .

It can be noticed that temperatures within the sample and in the holder are very close when no crystallization takes place. During the crystallization phase (approximately 5 min), the sample temperature becomes slightly higher than  $T_\infty$  because of the exothermic characteristic of the crystallizations. However, this maximum deviation ( $\Delta T_{\text{max}} \approx 0.7 \text{ K}$  on Fig. 3) remains small.

The corresponding thermogram is represented by a continuous line (“nominal values” curve) on Fig. 4. It also shows several thermograms calculated with different values of  $A$  and  $B$ . It shows that a calculated thermogram is much modified by a variation of  $B$  than by the same variation of  $A$ . Since the determination of  $A$  and  $B$  is carried out starting from the thermogram, one understands that the estimation is much more difficult and imprecise for  $A$  than for  $B$ . This difficulty does not seem to depend on the inversion method but rather on the fast variation of  $J(T)$  with the temperature which induces the very weak influence of  $A$  on the thermal phenomena. Finally, it can be noticed that the area of the peak is preserved in all the cases since it is directly proportional to  $mL$ .

#### 4. Genetic algorithm approach of the parameters estimation

The model detailed previously introduces several parameters which can be classified in two groups:

- (1) quantities that can be directly measured by DSC or by any classical method. This concerns the heat capacities  $C_L$  and  $C_S$ , the apparent latent heat of fusion  $L$ , the melting point  $T_F$ , as well as the density  $\rho$ ;
- (2) coefficients  $A$ ,  $B$  and the global  $HS$  coefficient. These parameters are generally difficult to estimate with accuracy by classical methods.

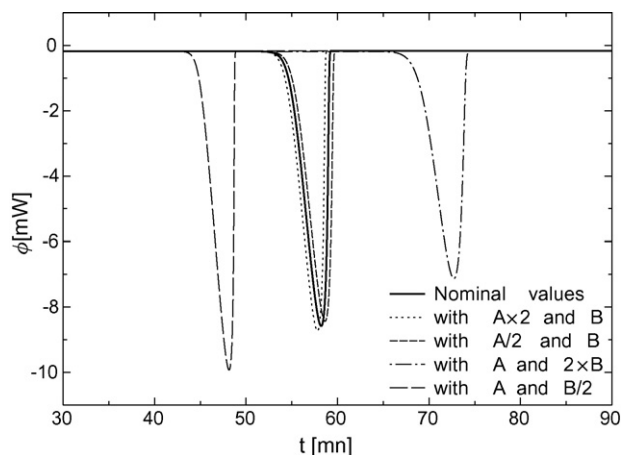


Fig. 4. Influence of parameters  $A$  and  $B$  on  $\phi(t)$ .

In this work, we consider the quantities of the first group as known and we use a “genetic algorithm” to estimate those of the second group. The sample amount as well as the cooling rate are selected in order to verify the temperature homogeneity assumption made in the model.

#### 4.1. Genetic algorithm method

A genetic algorithm (GA) is a method of stochastic optimization inspired by the biological evolution [22]. By analogy, a possible solution is called “individual” and all the individuals constitute a “population”. All the characteristics of an individual are encoded and stored in a “chromosome”. A numerical value called “fitness” ( $f$ ) is associated to each individual. It is a measurement of the “quality” of an individual which allows classification among themselves. Thus, an individual  $X$  is better than  $Y$  if  $f_X > f_Y$ .

GA iterative process begins with the creation of the “zeroth generation population” composed of  $N_{\text{ind}}$  randomly chosen individuals. The iterative process of evolution then begins (Fig. 5): the  $(g + 1)$  generation is deduced from the previous one according to the following consecutive steps:

- **Evaluation:** The chromosome of each individual is decoded and the corresponding fitness is calculated. At the end of this evaluation step, all the individuals of the initial population can be compared to each other.
- **Selection:** A subset of the initial population is selected. The  $N_{\text{ind}}/2$  individuals of this intermediate population are selected according to their fitness. Numerous methods exist [22], the objective being to obtain a good intermediate population while preserving the “genetic diversity”. In this work, we use the procedure of selection by tournaments where the best of two randomly chosen individuals of the initial population is added to the intermediate population. After  $N_{\text{ind}}/2$  tournaments, the intermediate population is complete.
- **Crossover:** Like in the nature, the crossover is one of the main processes of the evolution, during which the genetic information is exchanged between the individuals: two “parents” randomly chosen in the intermediate population gener-

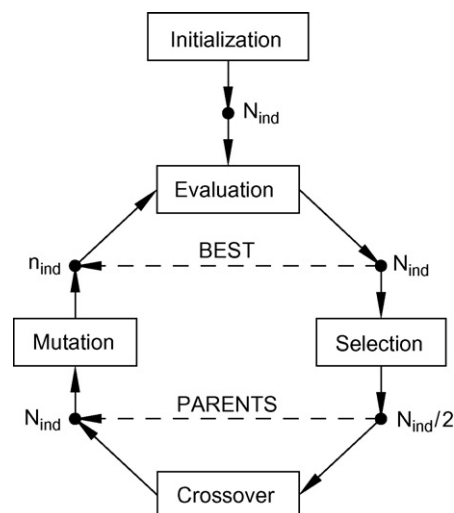


Fig. 5. GA optimization procedure.

ate two new individuals (i.e. the “children”). The crossover phase produces  $N_{\text{ind}}/2$  children who are added to the intermediate population. The resulting population is then of size  $N_{\text{ind}}$ .

- **Mutation:** “To mutate” an individual consists in randomly modifying the value of one of its genes. This mechanism allows to investigate the whole space of the solutions and so to avoid the convergence towards a local maximum. Mutation remains however a rare event and the probability  $p_{\text{mut}}$  that an individual undergoes a mutation during a generation is generally small.

A mechanism of elitism protects the best individual of every generation by ensuring that he appears unaltered in the next generation.

#### 4.2. Application to the thermophysical characterization of a freezing emulsion

As mentioned previously, unknown parameters are  $A$ ,  $B$  and  $HS$ , which constitute the chromosome of an individual.

In order to estimate an individual, we extract the values carried by its chromosome, which we use to calculate the thermogram as described in Section 3. The more the individual is “good”, the more this thermogram must approach the experimental thermogram. The fitness  $f$  associated to a particular individual is thus calculated by using:

$$f = - \int (\phi_{\text{exp}}(t) - \phi_{\text{sim}}(t))^2 dt \quad (9)$$

where  $\phi_{\text{exp}}(t)$  and  $\phi_{\text{sim}}(t)$  are, respectively, the measured and the calculated fluxes.

## 5. Results

The experimental results presented hereafter have been obtained from an “hexadecan within water” emulsion ( $\rho = 932.5 \text{ kg m}^{-3}$ ,  $T_F = 291 \text{ K}$ ), whose stability and thermal behaviour have been already examined [8,20]. Two samples have

Table 1  
Experimental specific heat capacity and latent heat energy

Quantity	Sample 1	Sample 2	Unit
$L$	112.5	114.3	$\text{kJ kg}^{-1}$
$C_L$	2300	2250	$\text{J kg}^{-1} \text{K}^{-1}$
$C_S$	1950	1880	$\text{J kg}^{-1} \text{K}^{-1}$

been used, with respective masses of 11.25 mg (sample 1) and 10.30 mg (sample 2). We used a Perkin-Elmer PYRIS DIAMOND differential scanning calorimeter (DSC). The value of the specific heat capacities ( $C_L$  and  $C_S$ ) and the latent heat energy are deduced from experimental thermograms using Perkin-Elmer Software. These values are gathered in Table 1.

As previously mentioned, the nucleation/crystallization probability is deduced from thermogram recorded during a steady cooling. Initial temperature is about 298 K and the cooling rate is  $-0.5 \text{ K min}^{-1}$ . This low value was selected after various tests in order to satisfy the assumptions of the model. Fig. 6 shows the corresponding experimental measurements.

A genetic algorithm is by definition a nondeterministic method. Thus, several identifications carried out with the same experimental data can not converge towards the same solution. The method is however useful if the obtained solutions are near.

To verify this point, we systematically made a series of 100 identifications for each sample. To exclude the cases of non convergences (detectable by a small adaptation value) we only kept the 50 better solutions. In each case, we fixed  $p_{\text{mut}} = 1\%$ ,  $N_{\text{ind}} = 256$ . The algorithm is stopped after 100 generations.

Table 2 gives the mean values onto this subset of the identified parameters, as well as the best obtained solution. First of all, it can be noticed that the best solution is very close to mean values, what shows that the method converges on near solutions. The strongest difference we can observe concerns the value of  $A$  for the second sample (about 12%). We still have this recurring difficulty to identify this coefficient.

If we consider now the best solutions for both samples, we observe an error about 3% between both values of  $B$ . This value being a characteristic of the dispersed phase, this good concordance is thus a proof of the capacity of the algorithm to identify this parameter. The difference between the values identified for  $A$  can seem important but could be explained again by its weak influence on the kinetics of the crystallizations and thus on the

Table 2  
GA results for samples #1 and #2

	Sample #1		Sample #2	
	Mean	Best	Mean	Best
$A$	$1.51 \times 10^4$	$1.52 \times 10^4$	$1.08 \times 10^4$	$0.95 \times 10^4$
$B$	$8.93 \times 10^5$	$8.93 \times 10^5$	$9.20 \times 10^5$	$9.15 \times 10^5$
$HS$	$4.52 \times 10^{-2}$	$4.42 \times 10^{-2}$	$5.64 \times 10^{-2}$	$6.44 \times 10^{-2}$

thermogram. However, this difference can also be related to the manufacturing process of the sample. Whereas the  $B$  coefficient only depends on the thermophysical properties of the dispersed phase, coefficient  $A$  linearly depends on the mean volume of the droplets. The emulsions being produced by mechanical agitation, the size distribution of the droplets can slightly vary from one sample to another, leading to different values of  $A$ . The factor 1.6 between the two values of  $A$  could thus come from a factor  $\sqrt[3]{1.6} \approx 1.2$  between the average diameters of the two samples, which is plausible.

The measured and calculated (with the best solution) thermograms for the two samples are represented in Figs. 7 and 8. One observes a good agreement between these thermograms. The emulsion being treated as monodisperse in the model, this good agreement between calculated and measured thermograms allows to affirm that the real emulsion can be considered as monodisperse too. The maximum shift is located at the beginning of the peak, i.e. at the beginning of crystallizations. Although the cooling rate is low and the sample small, this shift is probably related to the fact that the model does not take the conduction within the sample into account.

In comparison, the probability of crystallization was also determined with a classic method based on the direct analysis of the thermograms. This method, which supposes the equality between the temperature imposed by the calorimeter and that of the sample (isotherm), allows to determine the shape of  $J(T)$  without supposing a particular analytical form. It gives a set of couples  $\{T, J(T)\}$  which are drawn on Fig. 9. These curves show that, for a given sample, both methods give appreciably the same shape for  $J(T)$ . Supposing the mathematical form given by the Eq. (3), the corresponding values are, respectively,  $A = 9.93 \times 10^4 \text{ s}^{-1}$ ,  $B = 10.28 \times 10^5 \text{ K}^3$  for sample #1 and  $A = 6.62 \times 10^4 \text{ s}^{-1}$ ,  $B = 10.61 \times 10^5 \text{ K}^3$  for sample #2. It

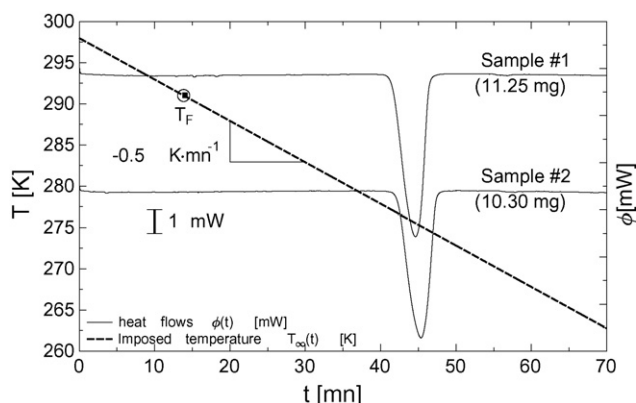


Fig. 6. Experimental thermograms.

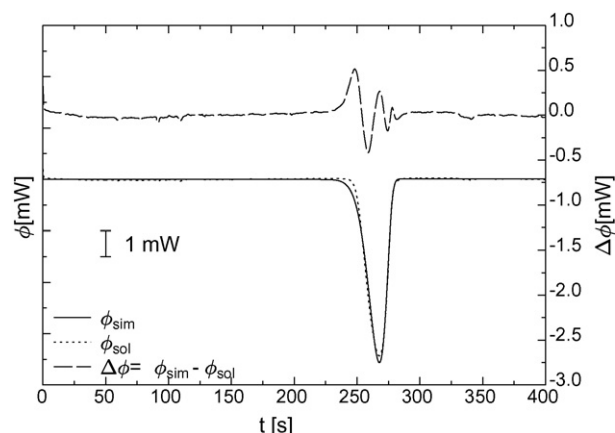


Fig. 7. Genetic algorithm best solution for sample 1.

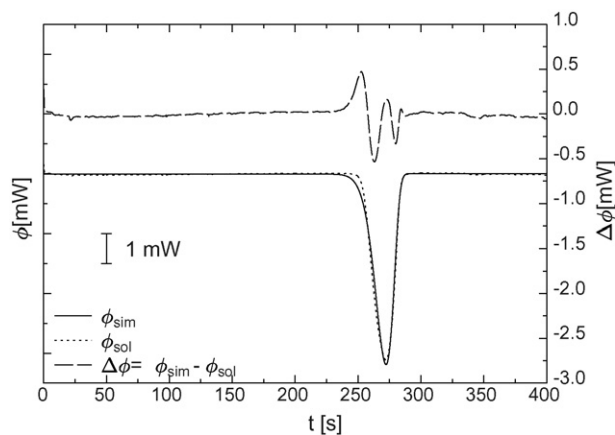


Fig. 8. Genetic algorithm best solution for sample 2.

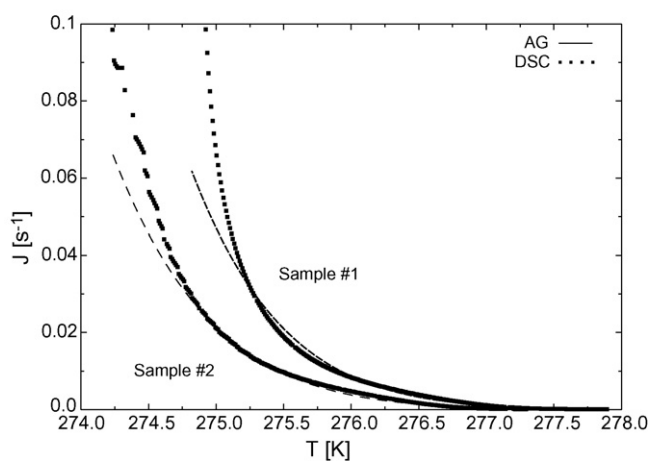


Fig. 9. Comparison of results.

can be also noted that the difference of values between the two methods can be due to the fact that the temperature of the sample is supposed to be equal to the temperature  $T_\infty$  in the classical method. However the useful information of the thermogram are limited to the part where crystallizations take place, that means where the error on the temperature of the sample is most important. Finally, the differences between results for both samples (mainly due to the  $A$  coefficient) are present whatever the method is. This fact tends to prove that it is not an artefact but a physical reality.

## 6. Conclusion

We presented a new method of determination of the crystallization probability from calorimetric measurement using a genetic algorithm. The use of a simplified thermal model has allowed to avoid several difficulties like the thermal conductivity measurement or the determination of the exact sample geometry.

The obtained results show the capacity of our method to estimate the crystallization probability. A first appreciation criterion is based on the identified  $B$  coefficients. Indeed, this coefficient only depends on the composition of the dispersed phase, and thus its value must be identical for two different samples with the same composition. In fact, it is what we observe, with an er-

ror about 3% between both samples. The analysis of the results about the coefficient  $A$  is much more delicate because its value depends on the distribution of the droplets sizes, which varies for each sample. Moreover, the influence of  $A$  on the crystallization kinetics being weak, its estimation is imprecise without any regard to the method.

The second criterion concerns the comparison of the values obtained by two different methods and for the same thermogram. We so compared the shape of the function  $J(T)$  obtained by our method with the “classic” calorimetric method. Again, the results are relatively close, in particular for the temperatures between 275 and 278 K, i.e. when crystallizations occur.

Several improvements are in development. The identification of the melting point  $T_F$  would allow to correct the possible calibration errors of the calorimeter. The exact influence of the shape of the sample on the thermal behaviour is also currently studied. If it is weak, we can try to improve the model by introducing the conduction. This will not only allow to work with faster cooling rate but also to try to estimate the thermal conductivity of the sample. Finally, the classic mathematical expression of  $J(T)$  used here, will be replaced by a spline representation.

However, the introduction of all these evolutions would increase the calculation time...

## References

- [1] V.P. Skripov, *Metastable Liquids*, John Wiley and Sons, New York, 1974.
- [2] H.R. Pruppacher, J.D. Klett, *Microphysics of Clouds and Precipitation*, D. Rigel Publishing Compagny, London, 1978.
- [3] M.A. Carrillo, C.A. Cannon, Supercooling point variability in the Indian meal moth, *Plodia interpunctella* (Hübner) (lepidoptera: Pyralidae), *J. Stored Prod. Res.* 41-5 (2005) 556–564.
- [4] D. Turnbull, *Phase Change*, Solid State Physics Acad. Press Inc. Publishers, 1956.
- [5] F.F. Abraham, A reexamination of the homogeneous nucleation theory: thermodynamic aspects, *J. Atomic Sci.* 25 (1968) 47–53.
- [6] J.A. Ehmimed, Y. Zéraouli, J.P. Dumas, A. Mimet, Heat transfers model during the crystallization of a dispersed binary solution, *Int. J. Thermal Sci.* 42 (2003) 33–46.
- [7] S. Gibout, J.P. Dumas, M. Strub, Identification of the nucleation probability in undercooled emulsions, *Proceedings of the 12th International Heat Transfer Conference*, Grenoble, France, 2002.
- [8] S. Gibout, M. Strub, J.P. Dumas, Estimation of the nucleation probability in emulsions, *Int. J. Heat Mass Transfer* 47 (2004) 63–74.
- [9] J.H. Perepezko, P.G. Höckel, J.S. Paik, Initial crystallization kinetics in undercooled droplets, *Thermochim. Acta* 388 (2002) 129–141.
- [10] P.W. Wilson, A.F. Heneghan, A.D.J. Haymet, Ice nucleation in nature: supercooling point (SCP) measurements and the role of heterogeneous nucleation, *Cryobiology* 46 (2003) 88–98.
- [11] L. Bosio, Surfusion et polymorphisme du gallium à la pression atmosphérique, *Métaux Corros. Indus.* 483 (1965) 432.
- [12] M. Akyurt, G. Zaki, B. Habeebullah, Freezing phenomena in ice-water systems, *Energy Convers. Manage.* 43 (2002) 1773–1789.
- [13] D. Clause, F. Gomez, C. Dalmazzone, C. Noik, A method for the characterization of emulsions, thermogravimetry: application to water-in-crude oil emulsion, *J. Colloid Interface Sci.* 287 (2005) 694–703.
- [14] E. Ruckenstein, Y. Djikaev, Recent developments in the kinetic theory of nucleation, *Adv. Colloid Interface Sci.* 118 (2005) 51–72.
- [15] D.H. Rasmussen, R. Appleby, Mary, G.L. Leedom, S.V. Babu, R.J. Naumann, Homogeneous nucleation kinetics, *J. Cryst. Growth* 64 (1983) 229–238.
- [16] D. Rasmussen, C. Loper, DSC a rapid method isothermal nucleation rate measurement, *Acta Metall.* 24 (1976) 117–123.

- [17] D. Clause, F. Gomez, I. Pezron, L. Komunjer, C. Dalmazzone, Morphology characterization of emulsions by differential scanning calorimetry, *Adv. Colloid Interface Sci.* 117 (2005) 59–74.
- [18] D. Kashchiev, N. Kaneko, K. Sato, Kinetics of crystallization in polydisperse emulsions, *J. Colloid Interface Sci.* 208 (1998) 167–177.
- [19] J.R. Avendaño-Gómez, R. Limas-Ballesteros, F. García-Sánchez, Modeling of trichlorofluoromethane hydrate formation in a w/o emulsion submitted to steady cooling, *Int. J. Thermal Sci.* 45 (2006) 494–503.
- [20] J.P. Dumas, Y. Zéraoui, M. Strub, M. Krichi, Models for the heat transfers during the transformations inside an emulsion. Part I. Crystallization of the undercooled droplets, *Int. J. Heat Mass Transfer* 37-5 (1994) 737–746.
- [21] M.J. Richardson, Quantitative aspects of differential scanning calorimetry, *Thermochim. Acta* 300 (1997) 15–28.
- [22] D.E. Goldberg, *Genetic Algorithms in Search, Optimization and Machine Learning*, Addison-Wesley, New York, 1989.